Supporting Information

HSC-Targeted Nanoplatform for Cascade-Responsive Imaging of Mitochondrial H_2O_2-Viscosity and Synergistic Melatonin-Based Antioxidant Therapy in Hepatic Ischemia-Reperfusion Injury

Yiru Wang,[†a] Yichen Liu,[†c] Yuting Sheng,[†a] Wen Zhang,[a] Xin Wang,[a] Hui Wang,[a] Wei Zhang[a] and Ping Li*[a,b]*

[a] College of Chemistry, Chemical Engineering and Materials Science, Collaborative Innovation Center of Functionalized Probes for Chemical Imaging in Universities of Shandong, Key Laboratory of Molecular and Nano Probes, Ministry of Education, Institutes of Biomedical Sciences, Shandong Normal University, Jinan 250014, Shandong, People's Republic of China

[b] College of Chemistry and Chemical Engineering, Northwest Normal University, Lanzhou 730070, People's Republic of China

[c] Aulin College, Northeast Forestry University, Harbin 150040, People's Republic of China

E-mail: lip@sdnu.edu.cn and zhangwen@sdnu.edu.cn

Table of Contents

Experimental Procedures

Reagents and Apparatus

Iodomethane, trimethylphenylindole, sodium acetate, and 4-formylphenylboronic acid pinacol ester were purchased from Shanghai Macklin Biochemical Technology Co., Ltd. All solvents were supplied by Sinopharm Chemical Reagent Co., Ltd. Soybean lecithin, cholesterol, vitamin A acid, nystatin, and LPS were from Shanghai Aladdin Biochemical Technology Co., Ltd. ELISA for p-AMPK, ACC2, and CPT1 were obtained from Jiangsu Enzyme Immunoassay Industrial Co., Ltd. MDA and α-SMA assay kits were purchased from Shanghai Tongwei Biotechnology Co., Ltd. ALT, AST, and BCA assay kits were provided by Elabscience Biotechnology Co., Ltd. UV-visible absorption spectra were recorded using a Thermo Scientific Evolution 220 spectrophotometer. Fluorescence spectra were measured with a Hitachi F-4700 fluorescence spectrophotometer. Cell viability was evaluated via CCK-8 assay using a Triturus microplate reader. Confocal fluorescence imaging was performed on a Leica SP8 high-resolution fluorescence microscope. The mass spectra were conducted with a Bruker Maxis ultra-high-resolution-TOF MS system. Proteomic analysis was performed by LC-MS/MS on a Thermo Fisher Q Exactive mass spectrometer. H&E-stained images were acquired using a Leica DM2500 optical microscope. ^{1}H NMR spectra were recorded at 400 MHz, and ^{13}C NMR spectra were recorded at 100 MHz with Bruker NMR spectrometers.

Preparation of ROS/RNS

$O_2^{\bullet-}$ was produced from KO_2 in dry DMSO by an ultrasonic method[1]. The concentration of $O_2^{\bullet-}$ was determined from the absorption at 250 nm (ε = 2682 M^{-1} cm^{-1}). 0.6 M $NaNO_2$, 0.6 M HCl, and 0.7 M H_2O_2 were added simultaneously to a 3 M NaOH solution at 0 ºC to get $ONOO^-$. The concentration of $ONOO^-$ was determined using the extinction coefficient of 1670 M^{-1} cm^{-1} at 302 nm in 0.1 M NaOH (aq.). H_2O_2 solutions were accessed by dilution of 30% hydrogen peroxide aqueous solution; the concentration was determined from the absorption at 240 nm (ε = 43.6 M^{-1} cm^{-1}). TBHP solutions were accessed by dilution of 70 % tert-butyl hydroperoxide aqueous solution. •OH was generated by the Fenton reaction of $FeCl_2$ with H_2O_2 (1:6) in deionized water. NO was obtained from a stock solution prepared with sodium nitroprusside. $^{1}O_2$ was prepared by the reaction of 10 mM of NaClO and 10 mM of H_2O_2 in PBS buffer solutions (pH = 7.4).

Synthesis

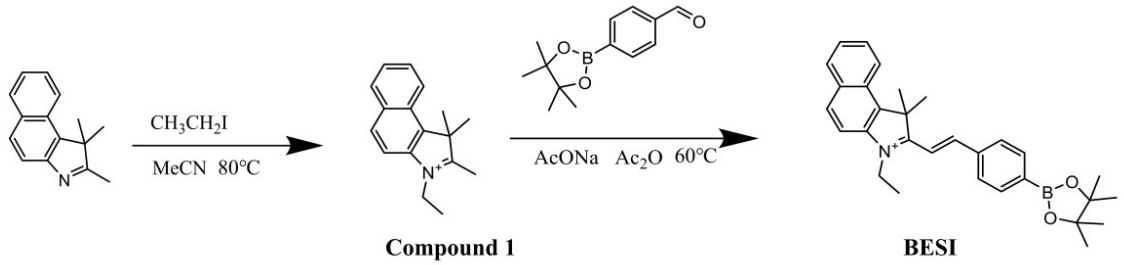

Scheme S1. The syntheses of BESI.

Synthesis of Compound 1. Compound 1 was prepared according to a reported method.[2-4] Trimethylphenylindole (9.6 mmol) and ethyl iodide (14.4 mmol) were dissolved in acetonitrile and refluxed at 80 °C for 24 hours. The mixture was then precipitated with diethyl ether to afford compound 1 (1.826 g, 7.6 mmol, 80%). HRMS data, m/z calculated for [$C_{17}H_{20}N^+$], 238.1591, found 238.1646. ^{1}H NMR (400 MHz, DMSO-d_6) δ 8.40 (d, J = 7.5 Hz, 1H), 8.32 (d, J = 8.9 Hz, 1H), 8.24 (d, J = 8.2 Hz, 1H), 8.19 (d, J = 8.9 Hz, 1H), 7.86 - 7.77 (m, 1H), 7.77 - 7.70 (m, 1H), 4.65 (q, J = 7.3 Hz, 2H), 2.97 (s, 3H), 1.78 (s, 6H), 1.52 (t, J = 7.3 Hz, 3H).

Synthesis of BESI. 4-Formylphenylboronic acid pinacol cyclic ester (316 mg, 1.36 mmol), sodium acetate (106 mg, 1.3 mmol), and compound 1 (472 mg, 1.3 mmol) were added to 10 mL of acetic anhydride, and the mixture was stirred at 60 ℃ for 8 hours. The crude product was purified by column chromatography, eluted with methanol/dichloromethane (1:15, v/v), dried by rotary evaporation, and filtered under vacuum to afford the deep red solid BESI (yield 50%). HRMS data, m/z calculated for [$C_{30}H_{35}BNO_2^+$]: 452.2756, found 452.2742. ^{1}H NMR (400 MHz, DMSO-d_6) δ 8.58 (d, J = 16.5 Hz, 1H), 8.47 (d, J = 8.3 Hz, 1H), 8.36–8.18 (m, 5H), 7.91–7.74 (m, 5H), 4.94 (q, J = 7.3 Hz, 2H), 2.07 (s, 6H), 1.57 (t, J = 7.3 Hz, 3H), 1.35 (s, 12H).

Synthesis of ATRA-BESI. 35 mg of soybean lecithin, 10 mg of cholesterol, and 5 mg of all-trans retinoic acid (ATRA) were dissolved in 20 mL of methanol, and sonicated until complete dissolution. Subsequently, 0.8 mg BESI was added to the solution and further treated with ultrasonication to ensure thorough dissolution. The mixture was concentrated under reduced pressure using a rotary evaporator until a uniform liposome film formed on the inner wall of the flask. After vacuum drying overnight, 2 mL of purified water was added for hydration, and the liposomes were uniformly dispersed in the aqueous solution via ultrasonication. Finally, the solution containing liposomes was sequentially filtered through 0.45 μm and 0.22 μm pore-size aqueous

microporous membranes (PVDF material), each for three times, ultimately obtaining a homogeneous liposome nanodispersion system.

Synthesis of ATRA-BESI-MEL. 35 mg of soybean lecithin, 10 mg of cholesterol, and 2 mg of all-trans retinoic acid were dissolved in 20 mL of methanol and ultrasonically treated until complete dissolution. Subsequently, 0.6 mg of BESI and 3 mg of MEL were added into the solution and sonicated until completely dissolved. The mixture was concentrated under reduced pressure using a rotary evaporator until a uniform liposome film formed on the inner wall of the flask. After vacuum drying overnight, 2 mL of purified water was added for hydration, and the liposomes were uniformly dispersed in the aqueous solution via ultrasonication. Finally, the solution containing liposomes was sequentially filtered through 0.45 μm and 0.22 μm pore-size aqueous microporous membranes (PVDF material), each for three times, ultimately obtaining a homogeneous liposome nanodispersion system.

Determination of encapsulation efficiency and drug loading capacity

After dissociation of liposomes using the solvent emulsion breaking method (80% methanol solution), the encapsulation efficiency (EE) was calculated according to the standard calibration curve of the free probe in the methanol-water system using the following formula:

EE=(total drug amount - free drug amount)/total drug amount × 100%.

In addition, the drug loading capacity (DL) is determined by the following formula:

DL=(drug mass/total carrier mass) × 100%

Selectivity evaluation

In the selectivity experiments (Fig. 1E), the BESI (10 μM) solution was treated with various analytes, including metal ions, ROS, RNS, and amino acids. The concentrations of each analytes were as follows: 1-25, Blank, 10 mM Na^+, 10 mM K^+, 1 mM Ca^{2+}, 100 μM Mg^{2+}, 1 mM Zn^{2+}, 100 μM Cu^{2+}, 100 μM Cu^+, 100 μM Al^{3+}, 100 μM Fe^{3+},100 μM Fe^{2+}, 10 μM $O_2^{\bullet-}$, 100 μM ClO^-, 100 μM $^1O_2$, 100 μM •OH, 100 μM NO, 100 μM $ONOO^-$, 100 μM His, 100 μM Cys, 100 μM Hcy, 100 μM GSH, 100 μM Arg, 100 μM Lys, 200 μM H_2O_2 and coexisting 200 μM H_2O_2 and 90% glycerol. The incubation time was 30 minutes at 37 °C. For the selectivity study of Fig. 1F, BESI was first incubated with 100 μM H_2O_2, followed by the addition of each interfering species (1-25): Blank, 10 mM Na^+, 10 mM K^+, 1 mM Ca^{2+}, 100 μM Mg^{2+}, 1 mM Zn^{2+}, 100 μM Cu^{2+}, 100 μM Cu^+, 100 μM Al^{3+}, 100 μM Fe^{3+},100 μM Fe^{2+}, 10 μM $O_2^{\bullet-}$, 100 μM ClO^-, 100 μM $^1O_2$, 100 μM •OH, 100 μM

NO, 100 μM $ONOO^-$, 100 μM His, 100 μM Cys, 100 μM Hcy, 100 μM GSH, 100 μM Arg,100 μM Lys, 200 μM H_2O_2 and coexisting 200 μM H_2O_2 and 90% glycerol. The incubation time was 45 minutes at 37 °C. Fluorescence spectra were measured using an excitation wavelength of 520 nm and an emission wavelength of 590 nm. All measurements were performed in triplicate, and the data represent the mean ± S.D.

Quantum yield determination of BESI

The fluorescence quantum yield of BESI was calculated using the comparative method described in previous publications[1], with crystal violet (CV) in methanol (Φ= 0.54) as the reference standard. The absorbance values of BESI and CV solutions at five different concentrations were measured, followed by the collection and integration of their fluorescence emission spectra. The quantum yield was calculated using the equation:

$$\Phi_{f,\,sam} = \Phi_{f,\,ref} \times (n_{sam}^2 / n_{ref}^2)\,(K_{sam} / K_{ref})$$

Where $\Phi_{f,\,sam}$ and $\Phi_{f,\,ref}$ denote the fluorescence quantum yield of the sample and reference, respectively; K represents the slope of the integrated fluorescence intensity vs. absorbance plot; and n is the refractive index of the solvent.

Calculation of radiation and non-radiation decay coefficients

The radiative (k_r) and non-radiative (k_{nr}) decay coefficients were calculated using the fluorescence lifetime (τ) and quantum yield (Φ) based on the standard method described in the literature[5]:

$$k_r = \Phi/\tau$$

$$k_{nr} = 1/\tau - k_r$$

Cell culture

HL-7702, RAW264.7, and LX-2 cells were purchased from the Cell Bank of the Chinese Academy of Sciences (Shanghai, China). HL-7702, RAW264.7, and LX-2 cells were cultured in high-glucose DMEM supplemented with 10% fetal bovine serum, 1% penicillin, and 1% streptomycin (w v^{-1}) at 37 °C in a 5% CO_2 / 95% air MCO-15AC incubator (SANYO, Tokyo, Japan).

Cell viability assay

The cell counting kit-8 (CCK-8) assay was employed to assess the effects of BESI, ATRA-BESI, and ATRA-BESI-MEL on LX-2 cell viability. First, cells were seeded into 96-well plates, followed by the addition of different concentrations of BESI, ATRA-BESI, or ATRA-BESI-MEL. The wells were then incubated with the cells for 24 h. Subsequently, CCK-8 reagent (10 μL $well^{-1}$) was added.

After 2 h, the absorbance of the solution at 450 nm was measured using a Triturus microplate reader.

Cellular fluorescence imaging

Cells were seeded on 15 mm glass-bottom dishes and cultured for 24 h. The living cells were treated with different agents. Then, the cells were washed three times with 1.0 mL PBS before imaging. All the fluorescence images were obtained on a Leica SP8 high-resolution fluorescence microscope. The excitation wavelength of the BESI was 561 nm, and the corresponding red channel of 580-640 nm emission wavelength was collected. For the co-localization experiment, the imaging parameters were as follows: All collection windows were 500-520 nm with excitation at 488 nm for 75 nM MitoTracker Green, 75 nM LysoTracker Green, 100 nM EndoTracker Green, and 100 nM GolgiTracker Green. Each experiment was repeated at least three times with identical results.

Establishment of the hepatic ischemia−reperfusion injury model

At the cellular level, ischemia−reperfusion injury was simulated via oxygen-glucose-serum deprivation/reperfusion. LX-2 cells were subjected to ischemia by culturing in glucose-free and serum-free DMEM supplemented with deoxygenated sodium dithionite (0.15 mM) for 30 min. Reperfusion was induced by replacing the medium with standard high-glucose, serum-containing DMEM under 5% CO_2 and 95% O_2 conditions for 30 min.

In the mouse model, a 70% partial hepatic ischemia−reperfusion injury (HIRI) model was established in 6-week-old male C57BL/6J mice via simulating liver surgery. The mice in the HIRI group were given a laparotomy to expose the liver, and the portal vein and hepatic artery of the median and the left lateral lobes were clamped with a microvessel clip for 1 h to induced 70 % partial hepatic ischemia. Subsequently, the vascular clamp was released for 1 h of reperfusion. Control mice underwent identical surgical procedures without vascular clamping. All mice were anesthetized during surgery. All in vivo experiments, including hepatic surgery in mice, were approved by the Ethical Committee of Shandong Normal University (Approval No. AEECSDNU2025159) and conducted in compliance with national regulations, international guidelines, and institutional standards at Shandong Normal University.

Fluorescence imaging experiments of mice

The experiments utilized 6-week-old C57BL/6J mice. All mice received intravenous injections of

ATRA-BESI (0.1 mg/g). The mice were anesthetized prior to injection and during imaging procedures. For the normal group, the liver was exposed as a control. During the laparotomy surgery, the mice were anesthetized by inhaling isoflurane. Images were gathered using the IVIS Lumina II in vivo imaging system with an excitation of 520 nm and an emission window of 570 ± 10 nm. All animal experiment methods were approved by the Animal Experiment Ethical Review Committee of Shandong Normal University (Approval No. AEECSDNU2025190) and conducted in compliance with national regulations, international guidelines, and institutional standards at Shandong Normal University.

Proteomic analysis

LKB1 (1.0 mg mL^{-1}) was incubated for 3 h at 37 °C in buffer (10 mM PBS, pH 7.4) supplemented with 1 mM H_2O_2. Samples were lyophilized, digested with trypsin, and peptides were purified via C18 solid-phase extraction. LC-MS analysis was performed on a Q Exactive mass spectrometer, and data were analyzed using MASCOT software.

Hematoxylin and eosin staining of major organs

The tissue samples were fixed with 4% paraformaldehyde and dehydrated, embedded, sectioned, and stained with hematoxylin and eosin. Finally, the sections were imaged through an optical microscope (Leica, DM2500).

Assessment of intracellular ROS level

ROS levels in LX-2 cells were measured using a commercial ROS indicator DCFH-DA. Cells were incubated with 15 μM DCFH-DA at 37 °C for 30 minutes, followed by fluorescence imaging and measurement of fluorescence intensity. The excitation wavelength was 488 nm, and the emission window was 490-550 nm.

Statistical analysis

The data for each group were accumulated from at least three independent experiments and expressed as the mean ± S.D.. For each experiment, unless otherwise noted, n represents the number of independent replicates per experiment. The Student's t-test was used for comparisons between two groups of experiments. Statistically significant P values are indicated in the Figures and legends as ***$P < 0.001$, **$P < 0.01$.

Supplemental Table and Figures

Table S1. Photophysical data of H_2O_2-activated BESI in low and high viscosity environments.

Solvents	Φ[a]	τ[b](ns)	radiative decay rate constant (s^{-1})	nonradiative decay rate constant (s^{-1})
0% Glycerol	0.015	0.472	3.178×10^7	2.087×10^9
90% Glycerol	0.14	0.563	2.487×10^8	1.528×10^9

[a] fluorescence quantum yield; [b] fluorescence lifetime; $k_r = \Phi/\tau$ (radiative decay coefficients); $k_{nr}=1/\tau - k_r$ (nonradiative decay coefficients). Data were recorded in glycerol/PBS at 25 °C after incubation with 100μM of H_2O_2.

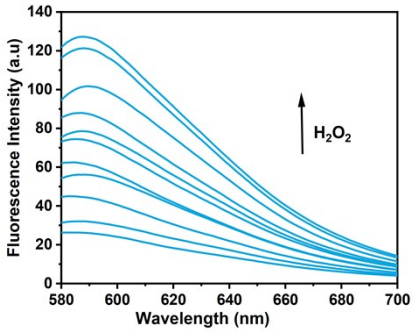

Fig. S1. Fluorescence response of BESI (10 μM) in the presence of H_2O_2 (0-200 μM) at various concentrations. $\lambda_{ex/em}$=520/590 nm.

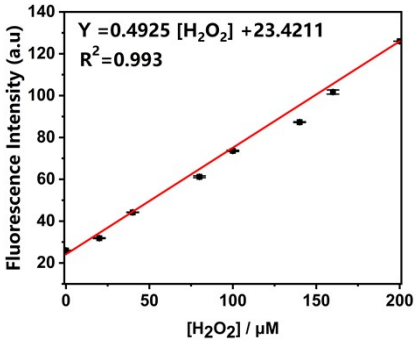

Fig. S2. The linear relationship between fluorescence intensity of BESI (10 μM) and H_2O_2 concentrations (0-200 μM). $\lambda_{ex/em}$=520/590 nm. The data are expressed as the mean ± S.D. (n = 3 independent experiments).

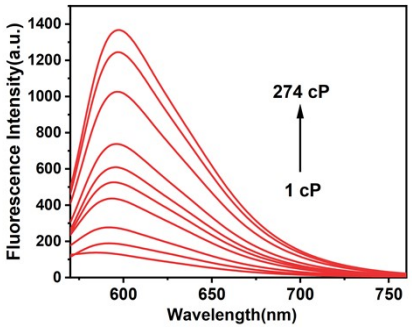

Fig. S3. Fluorescence response of H_2O_2-activated BESI (10 μM) in environments of varying viscosities. λ_{ex}=520 nm.

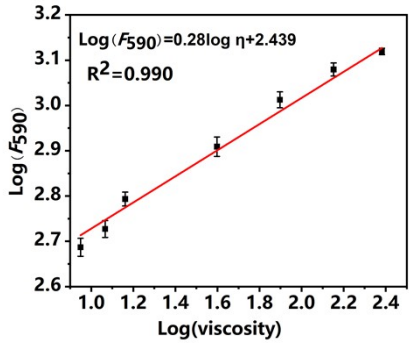

Fig. S4. A linear relationship between log F_{590} of H_2O_2-activated BESI (10 μM) and log viscosity (1 cP-274 cP). $\lambda_{ex/em}$=520/590 nm. The data are expressed as the mean ± S.D. (n = 3 independent experiments).

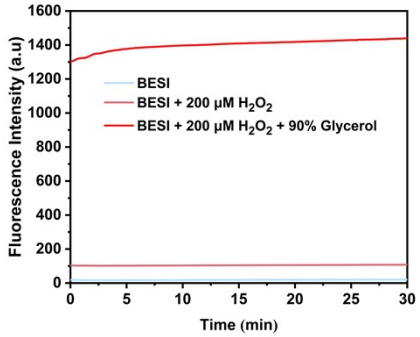

Fig. S5. Time course of fluorescence changes of 10 μM BESI in PBS buffer, H_2O_2 (200 μM), or H_2O_2 (200 μM) coexisting with 90% glycerol. $\lambda_{ex/em}$=520/590 nm.

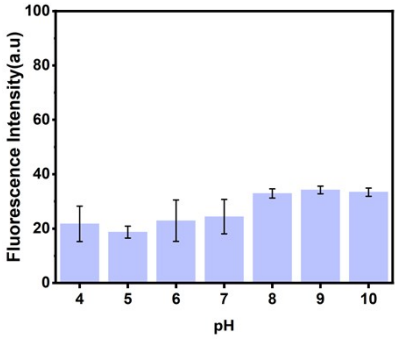

Fig. S6. Fluorescence of BESI (10 μM) at different pH values. $\lambda_{ex/em}$=520/590 nm. The data are expressed as the mean ± S.D. (n = 3 independent experiments).

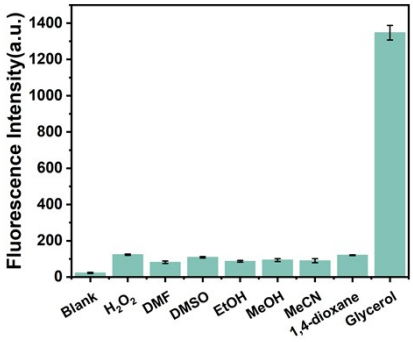

Fig. S7. Fluorescence of BESI (10 μM) in different polar solvents (Blank, 200 μM H_2O_2, DMF, DMSO, EtOH, MeOH, MeCN, 1,4-dioxane, and coexisting 200 μM H_2O_2 and 90% glycerol). $\lambda_{ex/em}$=520/590 nm. The data are expressed as the mean ± S.D. (n = 3 independent experiments).

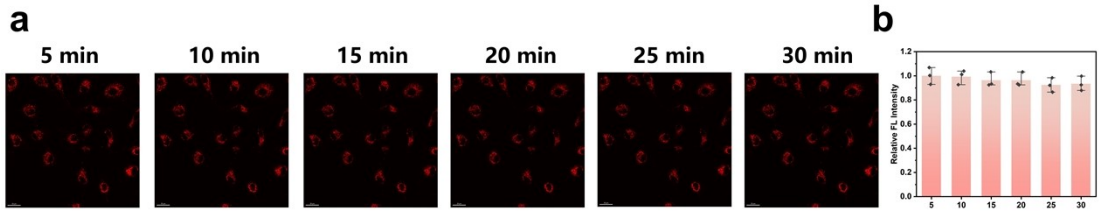

Fig. S8. The photostability of BESI in LX-2 cells. (a) LX-2 cells incubated with 2 μg/mL LPS for 3 hours were subjected to fluorescence imaging, with BESI (15 μM) added 30 minutes before imaging. (b) Relative fluorescence intensity output of a. λ_{ex}=561 nm, λ_{em}=580-640 nm. The data are expressed as the mean ± S.D. (n = 3 independent experiments).

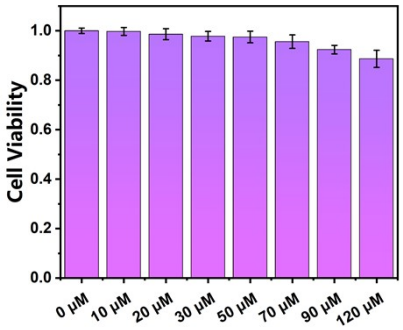

Fig. S9. Cell viability of BESI towards LX-2 cells with an incubation time of 12 h. The data are expressed as the mean ± S.D. (n = 3 independent experiments).

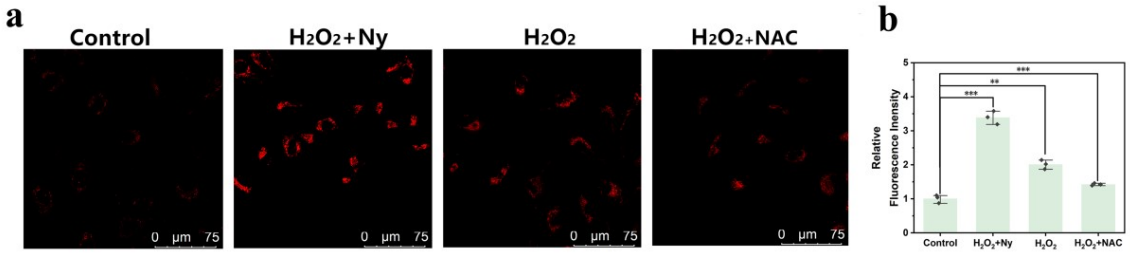

Fig. S10. Fluorescence imaging of living HSC. (a) Cascade-responsive fluorescence imaging in LX-2 cells pre-incubated with 15 μM BESI under different treatments: Control, 200 μM H_2O_2 + 20 μM nystatin (Ny), 200 μM H_2O_2, and 200 μM H_2O_2 + 1 mM N-acetyl-L-cysteine (NAC). (b) Relative fluorescence intensity output of a. The data are expressed as the mean ± S.D. (n = 3 independent experiments). **P < 0.01, ***P < 0.001.

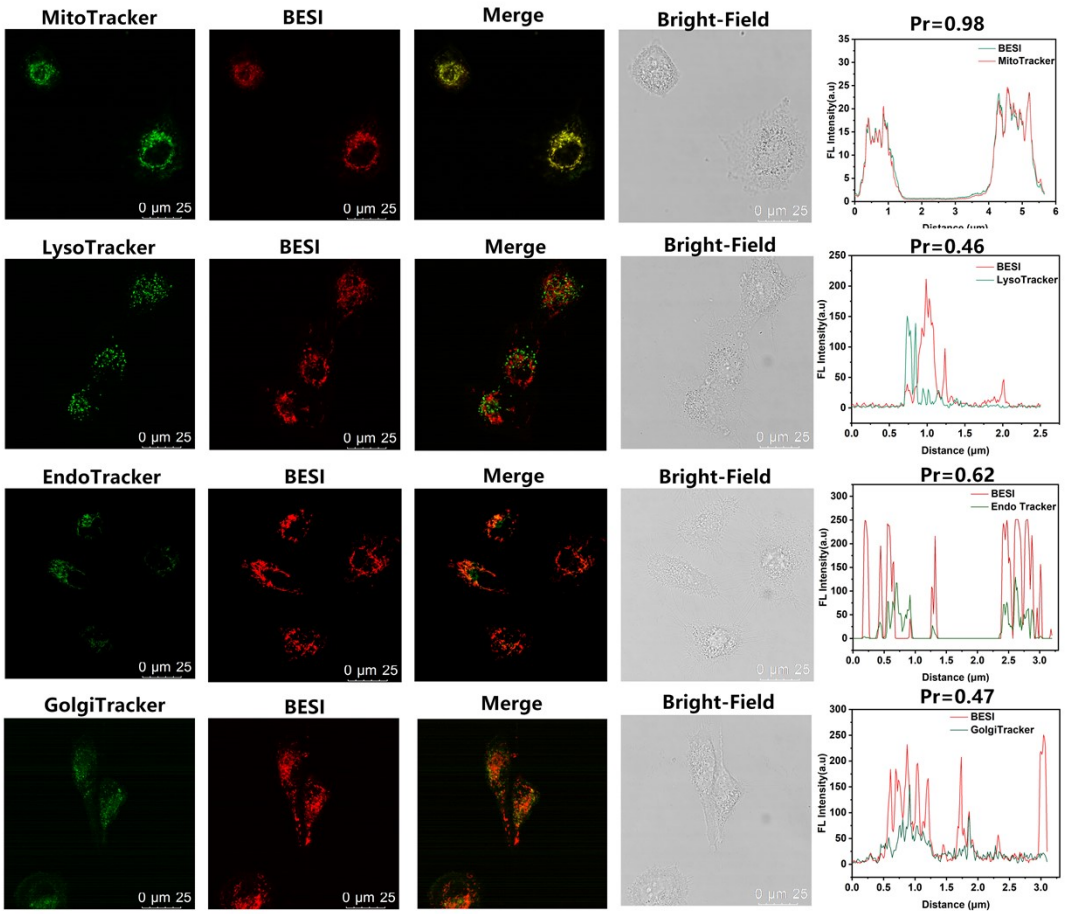

Fig. S11. Fluorescence imaging of LX-2 cells co-incubated with 15 μM BESI and commercial organelle green fluorescent dyes. All collection windows were 500-520 nm with excitation at 488 nm for 75 nM MitoTracker Green, 75 nM LysoTracker Green, 100 nM EndoTracker Green, and 100 nM GolgiTracker Green.

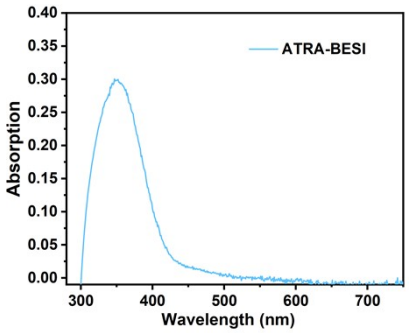

Fig. S12. The absorption spectrum of 90 ng/mL ATRA-BESI in 10 mM PBS buffer

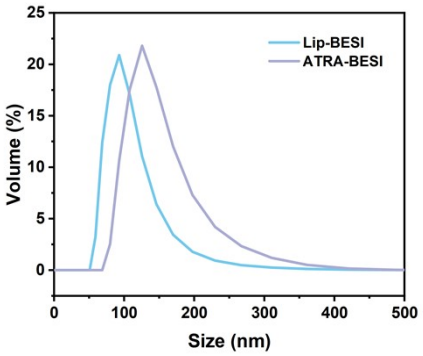

Fig. S13. Particle size distribution of ATRA-BESI and Lip-BESI in aqueous solution.

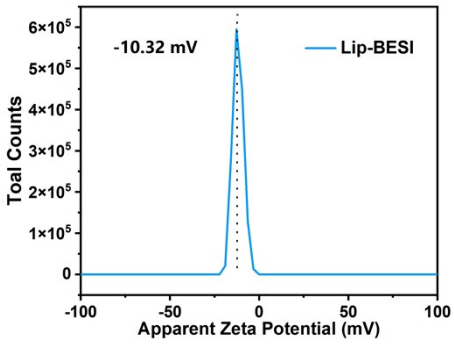

Fig. S14. Zeta potential distribution of Lip-BESI.

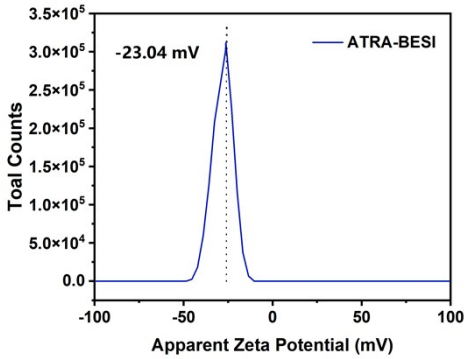

Fig. S15. Zeta potential distribution of ATRA-BESI.

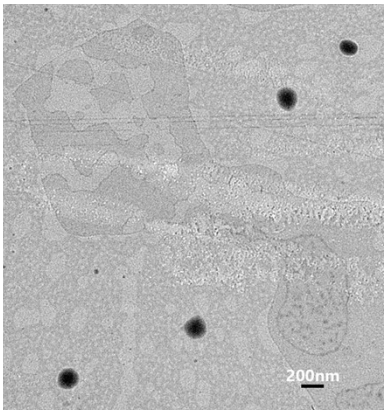

Fig. S16. Low-magnification transmission electron microscopy image of ATRA-BESI.

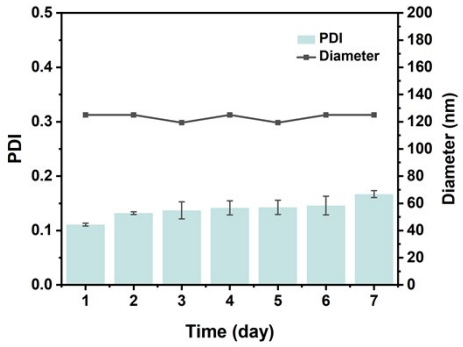

Fig. S17. The particle size and PDI of ATRA-BESI in aqueous solution over 7 days. The data are expressed as the mean ± S.D. (n = 3 independent experiments).

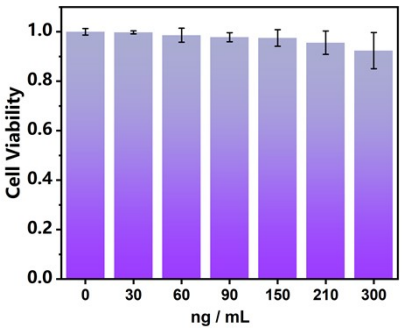

Fig. S18. Cell viability of ATRA-BESI towards LX-2 cells with an incubation time of 12 h. The data are expressed as the mean ± S.D. (n = 3 independent experiments).

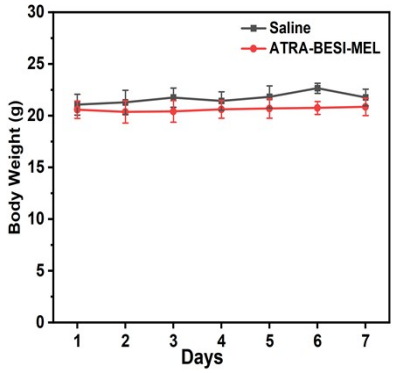

Fig. S19. Effect of ATRA-BESI (150 μM) and saline on the body weight of mice over two weeks. The data are expressed as the mean ± S.D. (n = 3 independent experiments).

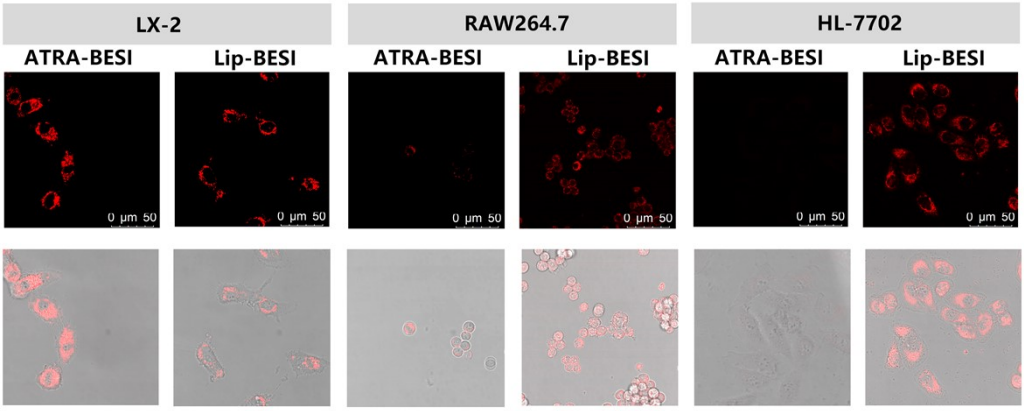

Fig. S20. Imaging of LX-2, HL-7702, and Raw 264.7 cells pre-stimulated with 2 μg/mL LPS for 3 h, followed by co-incubation with 20 μM ATRA-BESI or Lip-BESI for 30 minutes. The red channel excitation wavelength was 561 nm, with collection at 580–640 nm. The data are expressed as the mean ± S.D. (n = 3 independent experiments).

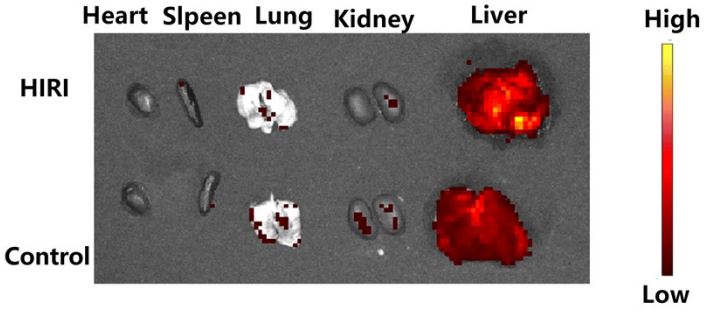

Fig. S21. In vivo fluorescence images of major organs dissected from mice.

Fig. S22. H&E staining of liver tissues.

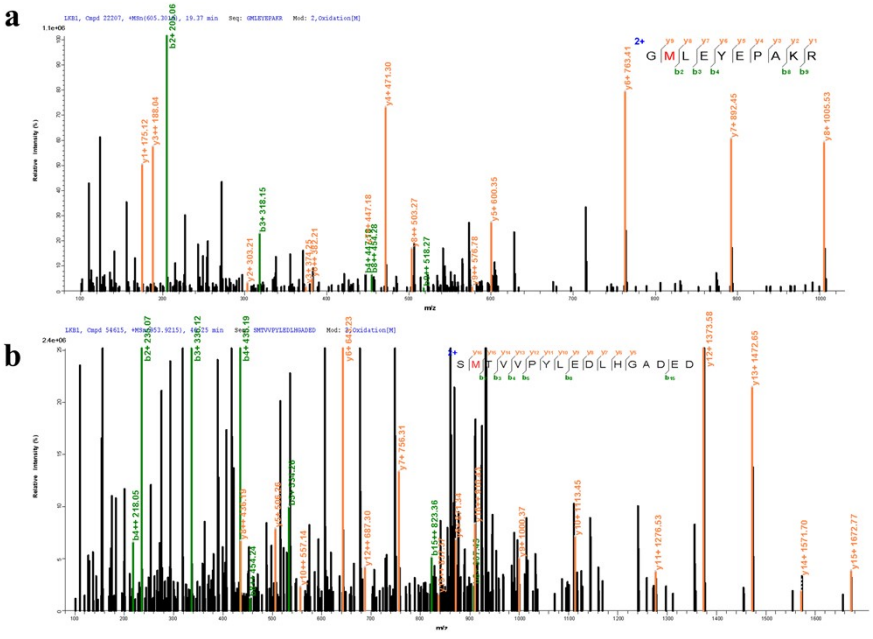

Fig. S23. Proteomic analysis of the reaction of LKB1 with H_2O_2 through LC-MS/MS. Amino acids labeled with red color denote modification by H_2O_2.

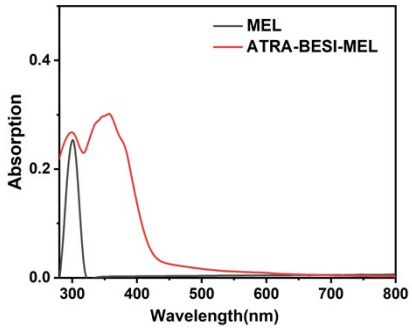

Fig. S24. The absorption spectra of ATRA-BESI-MEL and MEL.

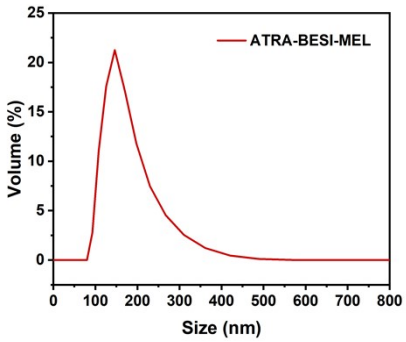

Fig. S25. Particle size distribution of ATRA-BESI-MEL in aqueous solution.

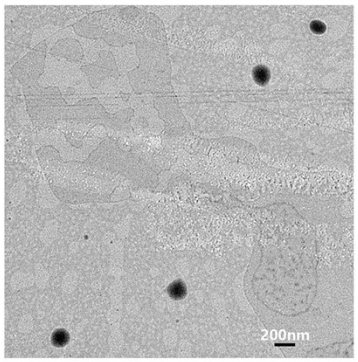

Fig. S26. Low-magnification transmission electron micrograph of ATRA-BESI-MEL.

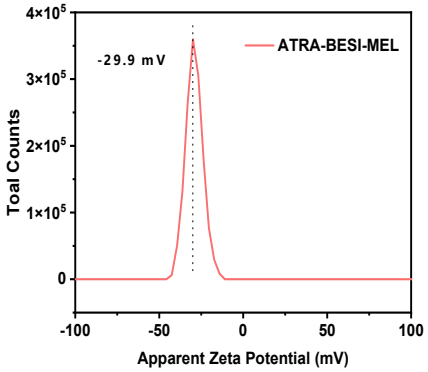

Fig. S27. Zeta potential distribution of ATRA-BESI-MEL in aqueous solution.

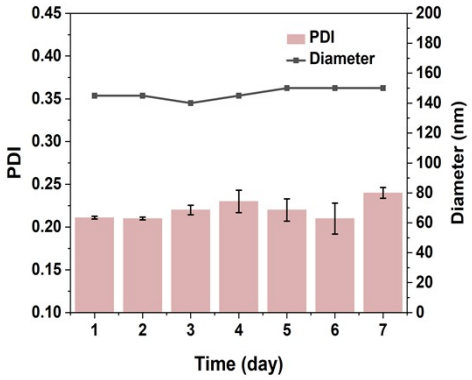

Fig. S28. Polydispersity index (PDI) and particle size determination of ATRA-BESI-MEL in aqueous solution over 7 days. The data are expressed as the mean ± S.D. (n = 3 independent experiments)

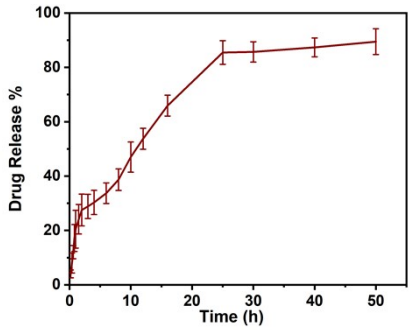

Fig. S29. The drug release curve of ATRA-BESI-MEL in 10 mM PBS Buffer at pH=7.4. The data are expressed as the mean ± S.D. (n = 3 independent experiments).

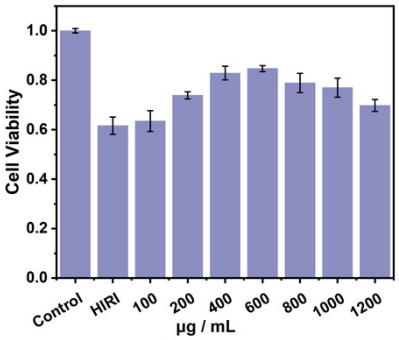

Fig. S30. The assessment of cell viability in LX-2 cells subjected to IR treated with different concentrations of ATRA-BESI-MEL. The data are expressed as the mean ± S.D. (n = 3 independent experiments).

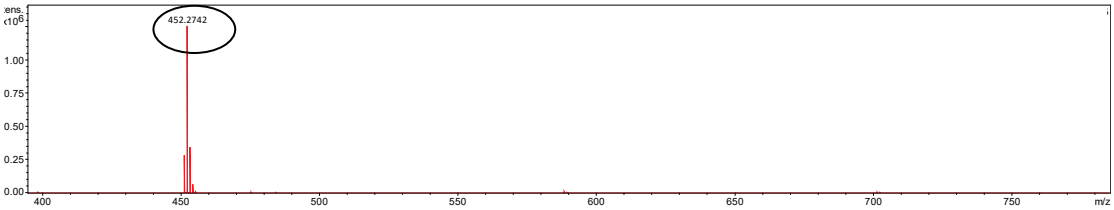

Fig. S31. HRMS of the BESI.

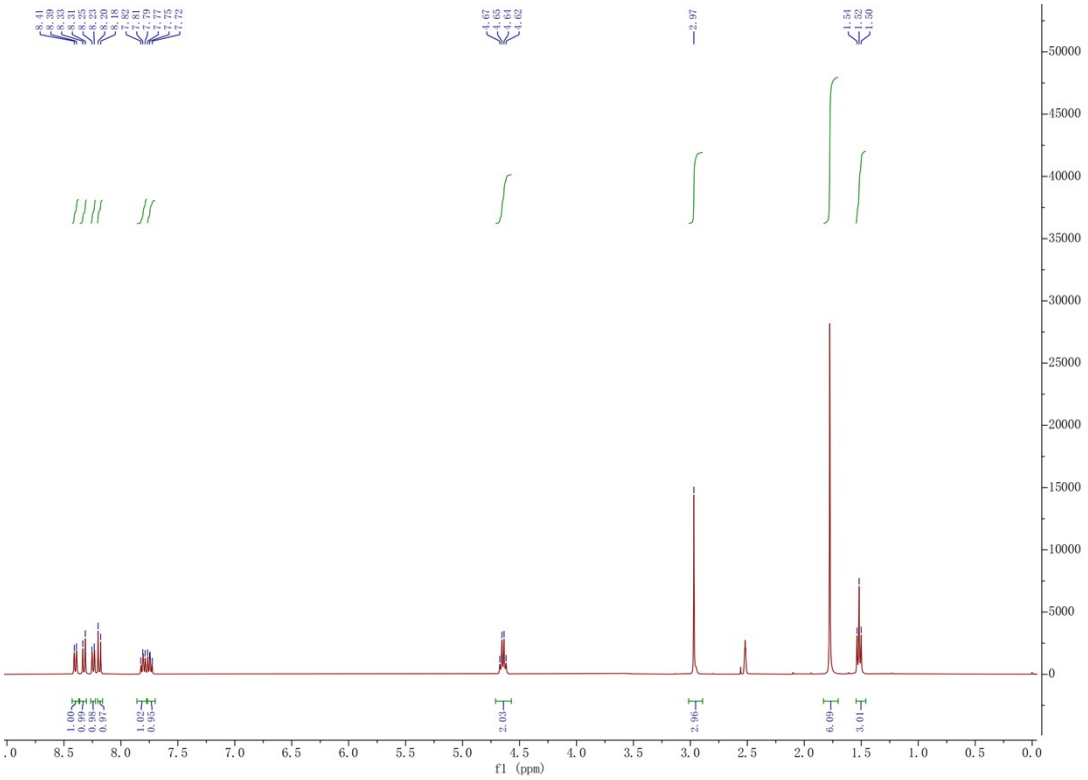

Fig. S32. ^{1}H NMR (400 MHz, DMSO-d_6) of compound 1.

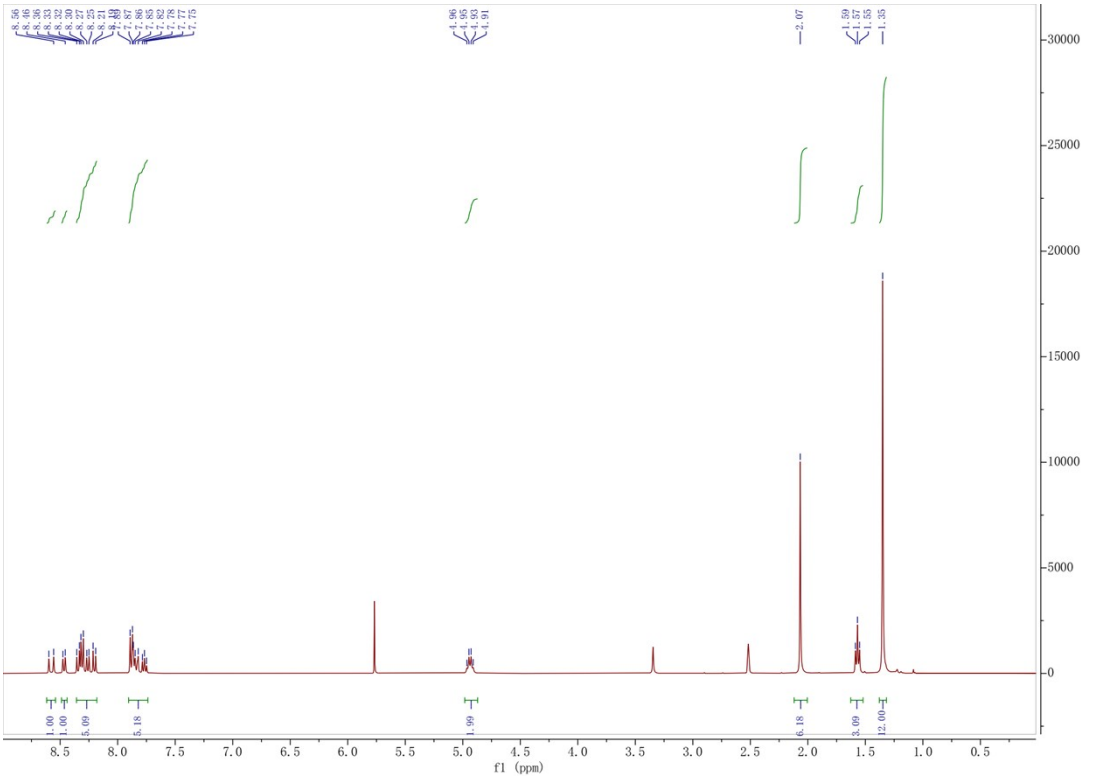

Fig. S33. ^{1}H NMR (400 MHz, DMSO-d_6) of the BESI.

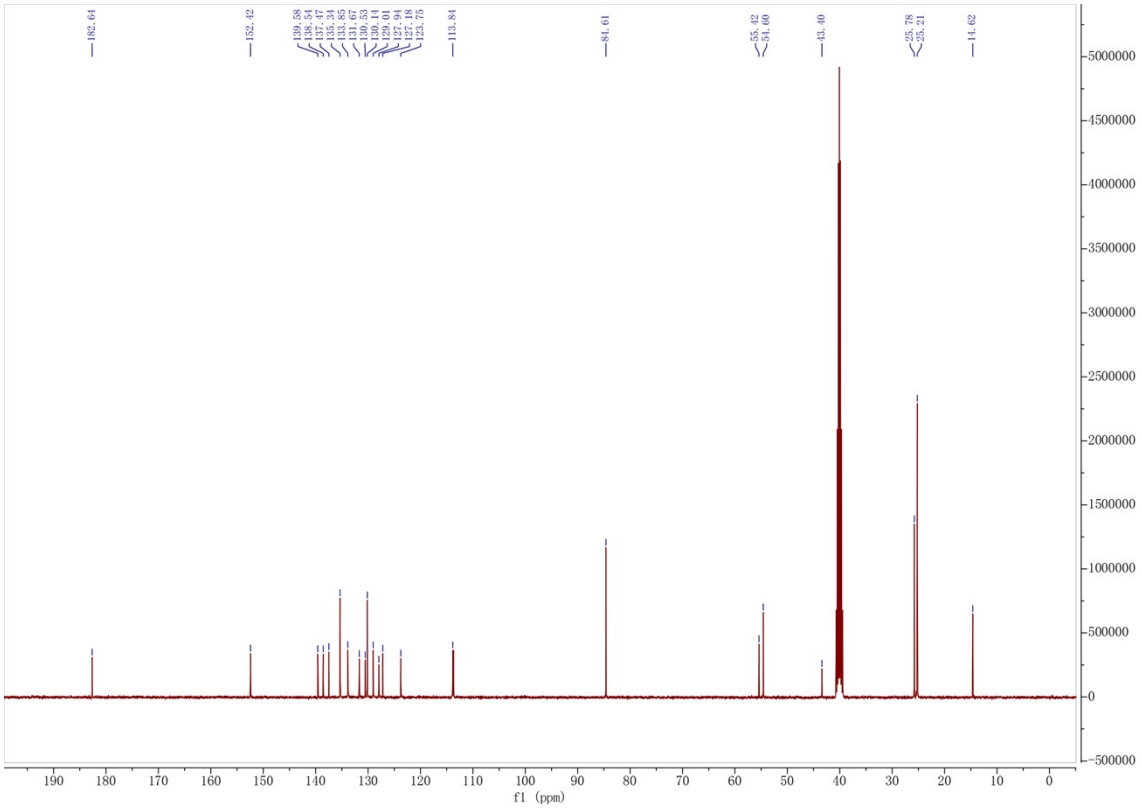

Fig. S34. ^{13}C NMR (100 MHz, DMSO-d_6) of BESI.

References

1 J. Liu, W. Zhang, C. Zhou, M. Li, X. Wang, W. Zhang, Z. Liu, L. Wu, T. D. James, P. Li and B. Tang, *J. Am. Chem. Soc.,* 2022, **144**, 13586-13599.

2 H. Maeda, K. Yamamoto, Y. Nomura, I. Kohno, L. Hafsi, N. Ueda, S. Yoshida, M. Fukuda, Y. Fukuyasu, Y. Yamauchi. *J. Am. Chem. Soc.*, 2005, **127**, 68-69.

3 D. Oushiki, H. Kojima, T. Terai, M. Arita, K. Hanaoka, Y. Urano, T. Nagano. *J. Am. Chem. Soc.*, 2010, **132**, 2795-2801.

4 B. C. Chen, C. D. Li, J. Zhang, J. F. Kan, T. T. Jiang, J. Zhou and H. M. Ma, *Chem. Commun.,* 2019, **55**, 7410-7413.

5 X. Li, D. Xu, A. Wang, C. Peng, X. Liu and J. Luo, *Green. Energy. Environ.,* 2024, **9**, 1592-1600.